K. Shahim[1]
e-mail: kamal.shahim@epfl.ch

J.-M. Drezet

LSMX,
Ecole Polytechnique,
Fédérale de Lausanne,
Station 12, CH-1015, Lausanne, Switzerland

Bryn A. Martin
LHTC,
Ecole Polytechnique,
Fédérale de Lausanne,
Station 17, CH-1015, Lausanne, Switzerland

S. Momjian
University Hospitals of Geneva,
University of Geneva,
Rue Gabrielle-Perret-Gentil
41211 Genève 14, Switzerland

Ventricle Equilibrium Position in Healthy and Normal Pressure Hydrocephalus Brains Using an Analytical Model

The driving force that causes enlargement of the ventricles remains unclear in case of normal pressure hydrocephalus (NPH). Both healthy and NPH brain conditions are characterized by a low transparenchymal pressure drop, typically 1 mm Hg. The present paper proposes an analytical model for normal and NPH brains using Darcy's and Biot's equations and simplifying the brain geometry to a hollow sphere with an internal and external radius. Self-consistent solutions for the large deformation problem that is associated with large ventricle dilation are presented and the notion of equilibrium or stable ventricle position is highlighted for both healthy and NPH conditions. The influence of different biomechanical parameters on the stable ventricle geometry is assessed and it is shown that both CSF seepage through the ependyma and parenchymal permeability play a key role. Although very simple, the present model is able to predict the onset and development of NPH conditions as a deviation from healthy conditions. [DOI: 10.1115/1.4006466]

1 Introduction

The mechanism of ventricle dilatation in the case of normal pressure hydrocephalus (NPH) is still obscure. In NPH, the large ventricle enlargement suggests the existence of a high transparenchymal pressure gradient. Many numerical models hypothesize the existence of a large pressure gradient but the experimental data consistently confirm that the mean cerebrospinal fluid (CSF) pressure gradient is less than 1 mm Hg [1,2]. The ventricle enlargement in NPH has been likened often to a sponge shaped balloon where an elevated internal pressure is the origin of expansion. A mini pressure gradient should exist between the ventricles and the intracranial subarachnoid space (SAS) in normal and NPH brains. This mini-gradient, as postulated by other researchers, is necessary to maintain the equivalence between the CSF production by choroid plexus in the ventricles and the absorption into the venous sinuses [4,5]. Another aspect present in different models is to consider an abnormal phase difference in the pulsatile nature of CSF flow [6]. A difference in timing between the pulsatile wave in the SAS and the ventricles could act as a driving force for enlargement. However, no detectable pressure difference in the waves was found in several experimental studies [2,7,8]. Several studies have been carried out experimentally to elucidate the unclear mechanism of NPH [9–11]. Due to the difficulty in performing experimental studies, interest in analytical and numerical approaches has increased [12–14]. Among these approaches, Levine highlighted the role of interstitial fluid (ISF) absorption as a source of compliance in a spherical model of brain [15]. In brief, the numerical and analytical studies that apply or predict a pressure gradient larger than 1 mm Hg do not help answer the NPH unclear mechanism.

1.1 Intracranial Pressure Variation in the Cranium. In a clinical study with communicating or noncommunicating hydrocephalus patients, Stephensen [2] measured ICP over a 24 h period and found no detectable pressure difference between the ventricles and the SAS. In addition, no consistent differences were evidenced between all the waves due to cardiac or respiration cycles. In an experimental study, Penn et al. [8] did measurements before, during and after both acute and chronic hydrocephalus induced by intracisternal injection of kaolin in dogs. They could not either find pressure gradients between the ventricles, brain parenchyma, and SAS greater than the resolution of the sensors (0.5 mm Hg). The pulse pressure waves appeared identical and no differences in magnitude or timing of waveforms were obtained. A precise measurement of pressure gradient has not yet been obtained because of the technological limit, but it is widely accepted that it is lower than 1 mm Hg both in healthy and in NPH conditions. Considering the experimental evidence, it is therefore worthy to investigate the normal and pathological conditions under a low pressure gradient (<1 mm Hg) using theoretical analyses.

1.2 Compartmental Compliance of the Brain. The brain parenchyma is made of different components accounting for the compliance source in form of CSF flow, CSF absorption or drained elasticity which have been incorporated in a variety of compartmental models [16,17]. The brain consists of incompressible interstitial fluid (ISF), brain tissue namely white and gray matter, and blood capillaries. The brain tissue contains intracellular (encapsulated) and extracellular ISF. Due to the high amount of water within these regions, brain tissue behaves as nearly incompressible under applied loads with a high rate of deformation. However, extracellular ISF might move in long timescale pathologies and give a degree of compressibility to the tissue, known as drained elasticity. The arteries and veins ($\sim$10% of the total intracranial volume) can be compressed and might play a role in ventricular enlargement in pseudotumor cerebri [18]. Excluding this small effect of arteries and veins, the parenchyma provides little elasticity to abrupt deformation. However, in long term, the flow and absorption of ISF within the interconnected channels could be the primary compliance source [8,19].

Owing to the high degree of saturation, the large dilation of the ventricles reported in NPH can only be possible if the brain looses compliance and some CSF flows out. Hence, the relative pressure between intracranial CSF pressure (ICP) and the venous sinuses

[1]Corresponding author.

Contributed by the Bioengineering Division of ASME for publication in the Journal of Biomechanical Engineering. Manuscript received May 9, 2011; final manuscript received March 25, 2012; accepted manuscript posted March 29, 2012; published online April 27, 2012. Assoc. Editor: Stephen Klisch.

instead of the level of venous blood pressure is the prominent factor for ventricle enlargement. There is a delicate balance of Starling forces of hydrostatic and osmotic pressure across the brain capillaries [15,20]. The mentioned components together affect the pathophysiology of ventricular expansion. In case of an abnormal incidence; for example elevated relative ventricular pressure or reduced absorption, the relative compressibility of these components plays the major role. Assimilating the brain as a sponge, the poro-elastic characteristics of the brain tissue is notably of high importance and has been included in a variety of numerical and analytical models of hydrocephalus [15,18,21–23].

1.2 Motivation and Work Plan. In the present work, normal and NPH brain conditions are addressed with the help of an analytical approach based on a simplified geometry. The model is based on Levine's spherical approach [15] considering the CSF-parenchymal reabsorption (or CSF seepage) through the ventricles and is further extended to solve the large deformation poro-elastic problem that is required when considering large ventricle dilations. An analytical equation for the pressure difference between the pia and ventricles, i.e., for the transparenchymal pressure difference, is derived using Biot's theory. Ventricle or parenchyma geometrical stability condition, i.e., stable shape, is investigated as a function of the different biomechanical parameters; thus clarifying the mechanism of ventricle dilation under a tiny pressure gradient. Contrary to the previous studies where the ventricular pressure was the main focus, in the present study, the importance of CSF seepage towards the brain parenchyma is highlighted.

2 Model

The condition of brain parenchyma maintaining its shape while CSF is produced within the ventricles, flows away through the aqueduct of Sylvius and partly seeps through the ependyma is not studied well. Considering a healthy brain, all parameters including the pressures inside the ventricles and at the pia layer, the parenchyma permeability and ISF absorption coefficient are subject to change in a bounded range due to cerebral auto regulation. In a healthy brain, the parenchyma maintains its geometrical stability by coming back to its original shape after any perturbations. In our model, the ICP variation in healthy and NPH brains is calculated using Darcy's equation modified by an absorption term where an analytical solution is presented for pressure difference between the ventricles and pia. Then, Biot's model for a healthy and NPH brain is solved analytically and the stability condition for the healthy brain is sought. To solve the large deformation problem associated with large ventricle dilation encountered in NPH conditions, iterations, each of them corresponding to a small deformation problem, are carried out using the Biot's poro-elastic formulation and updating the geometry of the ventricle.

2.1 Analytical Approach. With the aid of the poro-elasticity equations modified by Starling's law, the interaction between CSF flow through the parenchyma and the ability of the parenchyma to deform is modeled on a simplified geometry. Similarly to Kaczmarek and Levine [15,24], the brain parenchyma is modeled as a thick porous spherical shell, enclosing a small, spherical ventricular system. The parenchyma is treated as a porous solid permeated with interstitial CSF and proper boundary conditions allow taking into account the CSF seepage through the ependyma.

2.2 Formulations. The formulation from Levine [15] who considered the seepage of CSF towards the parenchyma is further developed to solve the large deformation problem when large ventricle dilation occurs. The solid matrix consists of the extracellular and intracellular spaces which are not exchangeable when the brain is subject to mechanical stress. The fluid network is the interstitial fluid in the interconnected channels of the extracellular space. The mass and momentum conservations previously described in detail [15] are reported hereafter. The momentum equation for the solid part [25] or mechanical equilibrium reads:

$$\mathrm{div}(\boldsymbol{\sigma}) - \alpha\vec{\nabla}\mathrm{p(r)} = \vec{0} \tag{1}$$

where $\boldsymbol{\sigma}$ is the brain tissue stress, p represents the ISF pressure (ICP) and α is the Biot-Willis parameter which is considered as unity. The pressure is only a function of radial position r in parenchyma due to spherical symmetry. The fluid flow through the extracellular spaces is governed by Darcy's law:

$$\vec{\mathrm{v}}_{\mathrm{darcy}} = -\mathrm{k}_{\mathrm{darcy}}\vec{\nabla}(\mathrm{p(r)} - \mathrm{p}_{\mathrm{venous}}) \tag{2}$$

where $\vec{\mathrm{v}}$ is the average ISF velocity (m/s), $\mathrm{k}_{\mathrm{darcy}}$ is the permeability coefficient (m^4/N.s). Taking the divergence of Eq. (2) yields the first term of the mass balance for the ISF:

$$\mathrm{div}(\vec{\mathrm{v}}_{\mathrm{darcy}}) = -\nabla\cdot\left(\mathrm{k}_{\mathrm{darcy}}\vec{\nabla}(\mathrm{p(r)} - \mathrm{p}_{\mathrm{venous}})\right) \tag{3}$$

According to Starling's law, the exchange of ISF and blood venous system varies linearly with the difference between the ICP pressure and the venous pressure $\mathrm{p}_{\mathrm{venous}}$. Venous pressure is assumed to be uniform throughout the parenchyma. Thus, the amount of ISF absorbed by the blood venous system is:

$$\mathrm{v}_{\mathrm{abs}} = -\mathrm{k}_{\mathrm{abs}} \times (\mathrm{p(r)} - \mathrm{p}_{\mathrm{venous}}) \tag{4}$$

where $\mathrm{k}_{\mathrm{abs}}$($\mathrm{m}^2$/N.s) represents the absorption coefficient of the brain parenchyma. Finally, combining Eqs. (3) and (4) yield the CSF mass conservation:

$$\nabla\cdot\left(\mathrm{k}_{\mathrm{darcy}}\vec{\nabla}\mathrm{p(r)}\right) - \mathrm{k}_{\mathrm{abs}} \times (\mathrm{p(r)} - \mathrm{p}_{\mathrm{venous}}) = 0 \tag{5}$$

2.3 Geometry and Biomechanical Parameters. The unknowns of the problem are u(r), the radial component of displacement of the parenchyma, and p(r) the ISF pressure. The ependyma surface is supposed to be the sphere with radius $\mathrm{R_i}$ and the outer pia layer the sphere with radius $\mathrm{R_e}$. These two radii are deduced from the real geometry of a healthy human brain [26]. Brain tissue is treated as both homogenous and isotropic and exhibits a linear elastic stress-strain behavior defined by a shear modulus G and a Poisson's ratio ν. Normal pathways of CSF flow via the aqueduct of Sylvius to the SAS are not considered here. Figure 1 shows the geometry of the brain parenchyma with its simplified spherical representation where the inner ventricle

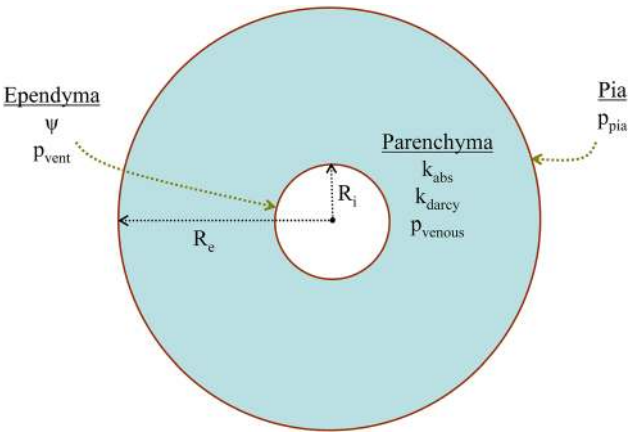

Fig. 1 Simplified spherical model of brain showing the parenchyma, ependyma and pia layer and associated biomechanical parameters

corresponds to the lateral and third ventricles. Equations (1) and (5) are solved for r varying between R_i and R_e. Four biomechanical parameters of the parenchyma are required; the absorption coefficient k_{abs}, the Darcy's permeability k_{darcy}, the shear elastic modulus G and the Poisson's ratio ν.

2.4 Boundary Conditions. The modeled ventricle is considered as fully permeable and can deform freely. Two boundary conditions are applied at the position of the ependyma, $r = R_i$, guaranteeing the continuity of fluid pressure through this membrane and taking into account the CSF seepage. Therefore, the first boundary condition consists of an applied pressure (Dirichlet condition):

$$p(r = R_i) - p_{venous} = p_{vent} \tag{6}$$

and the second boundary condition models the CSF seepage through the ependyma:

$$\left.\frac{\partial p}{\partial r}\right)_{r=R_i} = \frac{-\vec{v}\cdot\vec{n}}{k_{darcy}} = \frac{-\psi}{4\pi R_i^2 k_{darcy}} \tag{7}$$

where $\vec{n}$ represents the normal vector on the ventricle surface, ψ the amount of CSF seepage (positive quantity) and $-\psi/4\pi R_i^2$ is the radial velocity of CSF on the ventricular membrane. As this last boundary condition depends on the internal radius, R_i, iterations are required to obtain a self-consistent solution when ventricle dilation occurs, i.e., when R_i increases.

From a mechanical point of view, the total poroelastic pressure over the ventricle ($r = R_i$) is equal to the ventricle pressure [21,27]:

$$\boldsymbol{\sigma}_t \cdot \vec{n} = \boldsymbol{\sigma}\cdot\vec{n} - \alpha p = -p_{vent} \tag{8}$$

where $\boldsymbol{\sigma}_t$ and $\boldsymbol{\sigma}$ are the total and mechanical stresses, respectively and n represents the normal vector over the ventricle surface. Eventually, the outer layer of the brain parenchyma is assumed to be mechanically fixed thus imposing zero displacement:

$$u(r = R_e) = 0 \tag{9}$$

Please note that Eq. (1) comes from the small deformation poroelastic theory, i.e., Biot's theory. As the ventricle dilation can become rather large, solution for large deformations is obtained by iterating the small deformation solution and by updating the value of the ventricle radial position, R_i, notably in the expression of the flux associated with CSF seepage (cf. Eq. (7)). This way a self consistent large deformation poro-elastic solution is obtained. To get a stability condition, i.e., a condition in which the ventricle radial position, R_i, does no longer change, iterations are carried out until the displacement at the ventricle position becomes zero.

2.5 Analytical Solution. The analytical solution of pressure distribution takes the following form [15]:

$$p(r) - p_{venous} = \frac{A_1}{r}\sinh\left(\frac{r}{\sqrt{k}}\right) + \frac{A_2}{r}\cosh\left(\frac{r}{\sqrt{k}}\right) \tag{10}$$

where $k = k_{darcy}/k_{abs}$. The quantity $\sqrt{k}$ is a distance (meter unit) and represents the typical distance that ISF can flow within the parenchyma without being absorbed by blood vessels. Coefficients A_1 and A_2 are obtained from the boundary conditions:

$$\begin{aligned} A_1 &= \frac{d\times(p_{vent}-p_{venous}) - b\times(\partial p/\partial r)_{r=R_i}}{a\times d - b\times c};\\ A_2 &= \frac{a\times(\partial p/\partial r)_{r=R_i} - c\times(p_{vent}-p_{venous})}{a\times d - b\times c} \end{aligned} \tag{11}$$

where coefficients a, b, c and d are defined as follows:

$$\begin{aligned} a &= \frac{\sinh\left(\frac{R_i}{\sqrt{k}}\right)}{R_i};\quad b = \frac{\cosh\left(\frac{R_i}{\sqrt{k}}\right)}{R_i};\quad c = \frac{\cosh\left(\frac{R_i}{\sqrt{k}}\right)}{R_i\sqrt{k}} - \frac{\sinh\left(\frac{R_i}{\sqrt{k}}\right)}{R_i^2};\\ d &= \frac{\sinh\left(\frac{R_i}{\sqrt{k}}\right)}{R_i\sqrt{k}} - \frac{\cosh\left(\frac{R_i}{\sqrt{k}}\right)}{R_i^2} \end{aligned} \tag{12}$$

As the ISF pressure within the pia layer is close to the blood pressure in the cerebral veins [15], these two quantities are assumed to be equal:

$$p(r = R_e) = p_{pia} = \frac{A_1}{R_e}\sinh\left(\frac{R_e}{\sqrt{k}}\right) + \frac{A_2}{R_e}\cosh\left(\frac{R_e}{\sqrt{k}}\right) + p_{venous} \tag{13}$$

Using the expressions of A_1 and A_2, the pressure difference $\Delta p = p_{vent} - p_{pia}$ which corresponds to the transparenchymal pressure drop is given by:

$$\Delta p = \frac{\psi\sqrt{k}\times\tanh\left(\frac{R_e - R_i}{\sqrt{k}}\right)}{4\pi R_i^2 k_{darcy}\left[1 + \frac{\sqrt{k}}{R_i}\tanh\left(\frac{R_e - R_i}{\sqrt{k}}\right)\right]} \tag{14}$$

The transparenchymal pressure drop is proportional to the CSF seepage ψ meaning that only some CSF seepage is responsible for some pressure drop through the parenchyma. On the contrary to the expression of the fluid pressure, the expression of the radial displacement $u_r(r)$ is lengthy and detailed in the appendix while the stress and strain formulations are presented in their respective sections.

2.6 Input Data. In this section, the value for each parameter is given. Poisson's ratio and shear elastic modulus are taken as 0.3 and 3 kPa [28]. The permeability coefficient k_{darcy} for a healthy brain is taken as 10^{-11} m^4/N.s [23]. It is reported by Momjian (personal communication) that ISF seeps out of the parenchyma towards the SAS. To respect this condition, $\sqrt{k}$ should be of the order of $R_e - R_i$, i.e. 6 cm, that is to say $k_{abs} = 2.78\times10^{-9}$ m^2/N.s. As no values for this parameter are reported in the literature, k_{abs} is assumed to be in the range 10^{-11} to 10^{-8} m^2/N.s. The maximum production rate of CSF by the choroid plexus within the ventricles is reported to be around 0.6 ml/min, i.e., $\psi_{max} = 10^{-8}$ m^3/s, by Ref. [29]. In the present study, we consider that only part of this CSF can seep towards the parenchyma; thus ψ varies between zero and 10^{-8} m^3/s. Biot-willis parameter is taken as 1 neglecting the 10% portion of blood veins and vessels in the brain. Finally, the transparenchymal pressure drop Δp remains very low, typically 1 mm Hg, both in healthy and in NPH conditions. Table 1 summarizes the list of parameters with their values.

Table 1 Input parameters

ν (−)	G (Pa)	R_i (cm)	R_e (cm)	α (−)	Δp (mm Hg)	k_{darcy} (m^4/N.s)	k_{abs} (m^2/N.s)	ψ (m^3/s)
0.3	3000	2	8	1	1	10^{-11}	[10^{-11}–10^{-8}]	[0–10^{-8}]

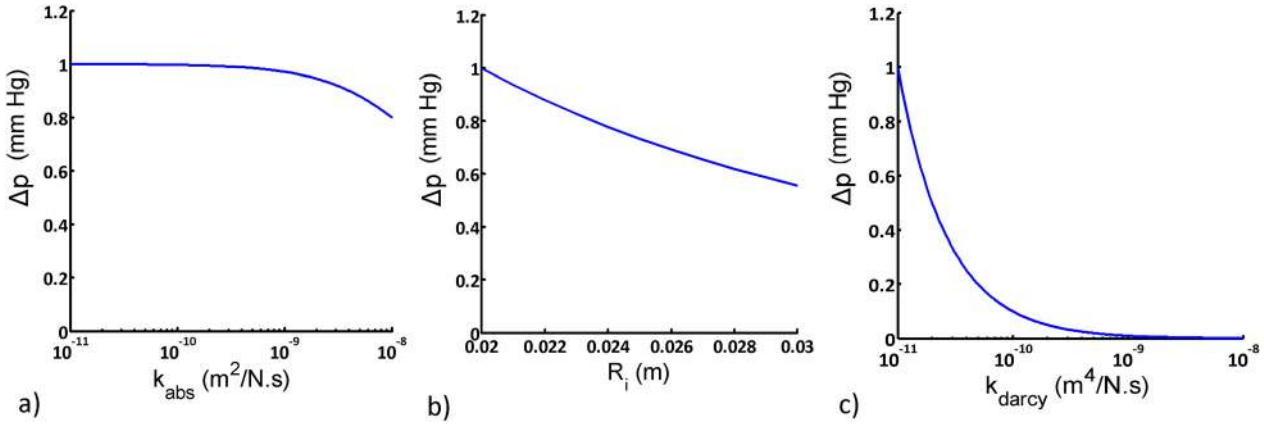

Fig. 2 Pressure drop in mm Hg when the absorption coefficient (*a*), internal radius (*b*) and permeability of parenchyma change

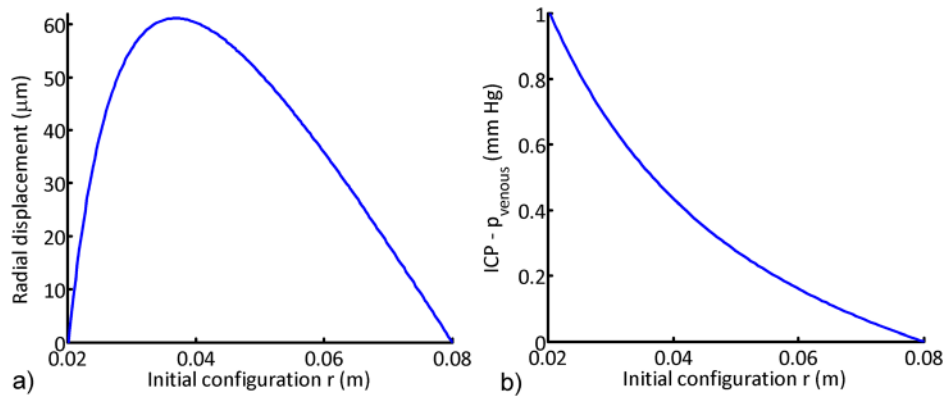

Fig. 3 (*a*) Radial displacement (μm) and (*b*) ISF pressure relative to the venous pressure (mm Hg) for a healthy brain with CSF seepage is 5% of total CSF production

3 Results

In this section, ICP and radial displacement results are shown for both healthy and NPH conditions. The influence of both CSF transependymal seepage ψ and absorption coefficient k_{abs} is studied. Equilibrium positions of the ventricle defined as $u_r(r = R_i) = 0$ are investigated for healthy and NPH brains.

3.1 Pressure Gradient. The transparenchymal pressure drop, Δp, defined in Eq. (14), is quantified separately for k_{darcy} varying in the range 10^{-11}–10^{-8} m^4/N.s, for R_i varying between 2 and 3 cm and for k_{abs} varying in the range 10^{-11}–10^{-8} m^2/N.s while keeping the remaining parameters fixed and equal to the values reported in Table 1 and fixing the CSF seepage ψ to 5.10^{-10} m^3/s. The results are shown in Fig. 2. Δp is a decreasing function of k_{darcy}, R_i and k_{abs}. Compared to the influence of R_i and k_{abs}, k_{darcy} has the strongest influence. Indeed, a decrease by an order of magnitude in k_{darcy} leads to a pressure drop divided by ten.

If for any reasons the CSF seepage, ψ, increases, a combined change of the three parameters can still keep the pressure gradient in a normal range, i.e., around 1 mm Hg. Among the three parameters, k_{darcy} plays a major role. This point is of high importance as ventricle dilation is reported to increase the permeability of the periventricular region [24].

3.2 Parenchyma Equilibrium Positions. In this section, the parenchyma equilibrium positions for healthy and NPH brains are sought. Mathematically speaking, this consists in searching R_i, the ventricle radius, that under imposed Δp and ψ yields a zero displacement, i.e., $u_r(R_i) = 0$. As previously explained, this requires the use of iterations to get a self consistent solution using Eq. (7) and to solve incrementally the large deformation problem that arises when R_i varies substantially as in the case of NPH. The solutions are provided for the pressure and displacement on the current configuration. In other words, r presents the Eulerian frame. As it is seen, both the pressure gradient (Δp) and the incremental displacement ($u_r(r)$) are functions of r; therefore, they are valid for any current configuration. The iterations start from the undeformed state or the healthy position ($r = R_i = 2$ cm) where the ventricle displacement at $r = 0.02$ m is zero, indicated as the first equilibrium position. The NPH equilibrium position is related to the case where the ventricle surface gets the second stable position with the enlarged state. The parameter variation is done in order to find the NPH situation where the pressure gradient in the current configuration is about 1 mm Hg and the ventricle surface displacement is zero. Meanwhile, the geometry (i.e., the internal radius R_i) as well as the CSF flux are updated to find the respective situations.

3.2.1 Healthy Brain. In a healthy brain, CSF seepage ψ and absorption coefficient k_{abs} should stay at a level that induces no ventricle wall movement; in other words, R_i should keep its value of 2 cm in our model. As no ventricle deformation takes place, k_{darcy} does not change either and stays at 10^{-11} m^4/N.s. Under a transparenchymal pressure drop of 1 mm Hg, the CSF seepage can reach a maximum of 5.10^{-10} m^3/s, i.e., 5% of ψ_{max}, while k_{abs} decreases slightly to 10^{-9} m^2/N.s to fulfill the condition of geometrical stability. The associated radial displacement and pressure profile through the parenchyma are reported in Fig. 3. The

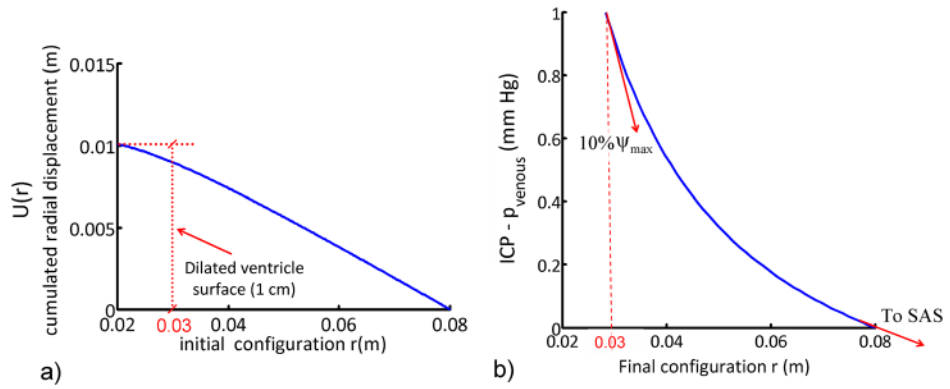

Fig. 4 (*a*) Cumulated radial displacement (m) versus initial radial position (initial configuration) and (*b*) fluid pressure (mm Hg) versus final radial position (deformed configuration) leading to a different stable position. The net ventricle wall dilation is sought to have the dilation of 1 cm.

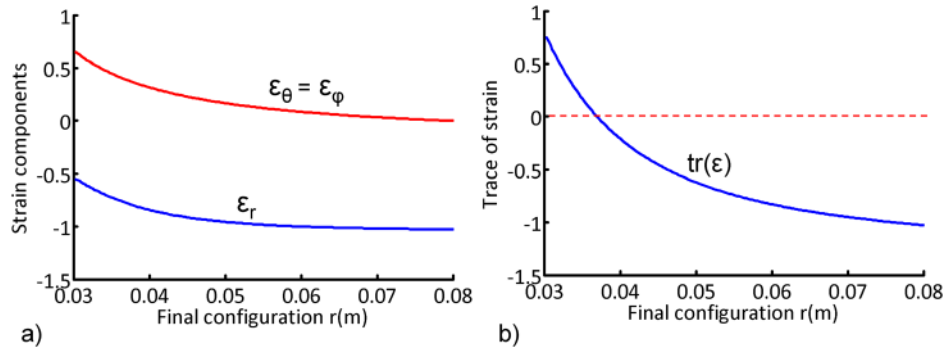

Fig. 5 (*a*) Radial strain ε_r and tangential strain ε_θ; (*b*) trace of strain tensor representing local volume change

parenchyma deforms very little with a maximum radial displacement of 60 μm but keeps its whole shape as the displacement at the inner radius, i.e.,. $u_r(r = R_i)$, is null. This case corresponds to a small deformation problem and no iterations are need as R_i does not change. The radial distribution of ICP presented in Fig. 3(*b*) shows that some of the ISF flows towards the SAS as the slope of pressure versus radial position is negative at $r = R_e$.

3.2.2 NPH Brain. With a further increase of CSF seepage ψ, ventricle wall diverts from stability resulting in positive displacement, leading to ventricle dilation and thus affecting substantially the permeability coefficient. This variation of ψ can be due to slow (chronic) or sudden (acute) changes in the brain condition. The situation corresponding to $\psi = 9.5\ 10^{-10} \approx 10\%\ \psi_{max}$ (10^{-9} m^3/s) is reported in Fig. 4 where the pressure drop is kept to 1 mm Hg, k_{abs} to 10^{-9} m^2/N.s and k_{darcy} to 10^{-11} m^4/N.s. In that case, the ventricle dilation amounts to 1 cm thus leading to a new equilibrium shape with $R_i = 3$ cm. Contrary to the situation of a healthy brain, the parenchyma deforms substantially with a maximum radial displacement of 1 cm. This requires the use of 250 to 300 iterations to get a converged solution at which the cumulated displacement (U(r)) corresponding to the large deformation problem is represented as a function of the original radial position. On the other hand, the pressure profile through the parenchyma is reported as a function of the final radial position, i.e., on the stable deformed configuration.

The large deformation of the parenchyma is mechanically characterized by the strain tensor. This one is calculated using the large deformation theory and owing to spherical symmetry, it is characterized by its radial component, $\varepsilon_r = 0.5\times((1+\partial u/\partial r)^2-1)$ and its tangential component, $\varepsilon_\theta = 0.5\times((1+u/r)^2-1)$. Both components are reported in Fig. 5(*a*) as a function of the radial location. The trace of the strain tensor is equal to $\varepsilon_r + 2\varepsilon_\theta$ in our spherical case. It yields the local volume change of a medium under deformation and is presented in Fig. 5(*b*). The periventricular region close to the ependyma is highly stretched tangentially whereas the remaining of the parenchyma becomes radially compressed. Notice that the tangential strain remains positive throughout the parenchyma.

3.3 k_{abs} Variation. The cumulated radial displacement and the pressure profile for a higher value of k_{abs}, 10^{-8} m^2/N.s, are shown in Fig. 6. One can see that an increase in the ability of blood vessels to absorb ISF leads to a less dilated ventricle and a slight reduction in the pressure drop. On the other hand, a decrease in k_{abs}, e.g. 10^{-10} m^2/N.s, has no influence on both the equilibrium position and the pressure profile as was already shown in Fig. 2(*c*).

3.4 k_{darcy} Variation. As reported by Ref. [24], Darcy's permeability value increases exponentially with local volumetric strain change, i.e., with the trace of the strain tensor. Although this last one is not uniform throughout the parenchyma as shown in Fig. 5(*b*), our model is valid only for uniform biomechanical parameters. Nevertheless, the high deformation of the NPH parenchyma (cf. Figure 4(*a*)) is going to lead to a substantial increase of k_{darcy}, thus of $\sqrt{k}$, and ΔP (Eq. (14)) becomes simply proportional to ψ/k_{darcy} for the range of k_{abs} retained in this study. This means that any increase of k_{darcy} has to be associated with an increase in ψ to maintain the transparenchymal pressure drop around 1 mm Hg. This is presented in Fig. 7 that shows the ventricle radial equilibrium positions as a function of the CSF seepage assuming that for ψ larger than 10% ψ_{max}, k_{darcy} increases linearly

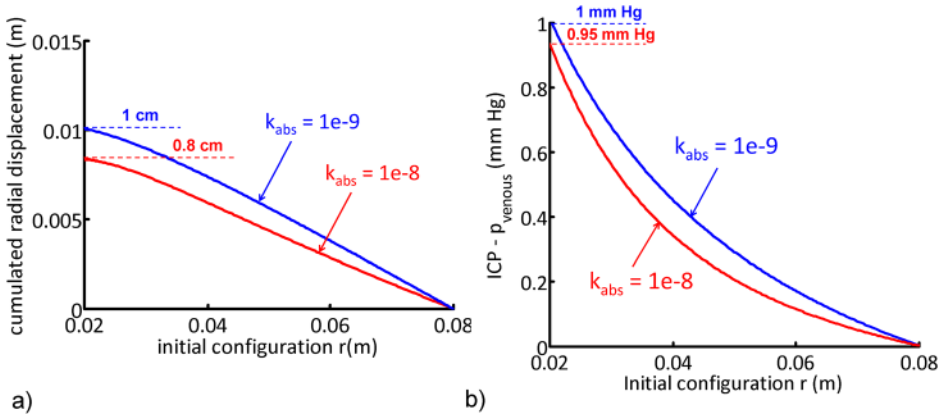

Fig. 6 Resulting cumulated radial displacement and fluid pressure in the parenchyma for two values of k_{abs} in m^2/Ns

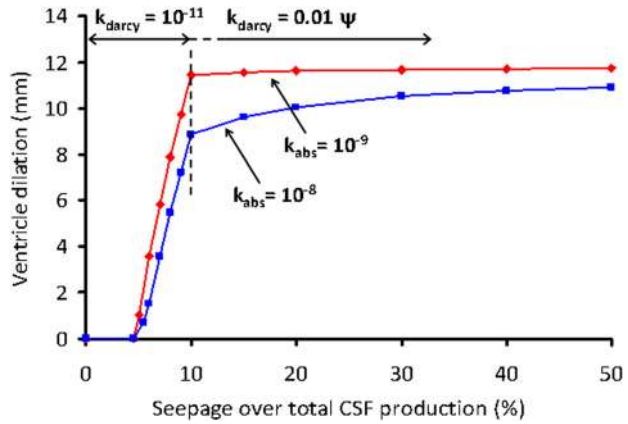

Fig. 7 Radial ventricle equilibrium position versus CSF seepage expressed in percentage of ψ_{max} for two absorption coefficients

with ψ. When ψ reaches ψ_{max}, k_{darcy} is equal to 10^{-10} $m^4/N.s$ and the ventricle dilation saturates to 3.2 cm. Figure 7 clearly delineates two regimes: first the transition from a healthy brain to a NPH brain due to a change in equilibrium position and second the NPH arrest owing to a substantial increase in both k_{darcy} and ψ. Notice that with the increase of the parenchymal permeability; all of the CSF production can seep into the parenchyma without leading to further dilation.

4 Discussion

In the present study, the analytical solution of Biot's equation over a simplified geometry inspired by the work of Levine [15] is further extended to determine the stable ventricle positions for both healthy and NPH brains. The simplification of the brain geometry is done in order to clarify the unknown mechanism of NPH onset and evolution and most important leads to the use of an analytical solution. The theoretical approach is based on the Levine's formulation which includes the ISF absorption by blood streams formalized by the Starling's law and possible CSF seepage through the ependyma. The transparenchymal pressure drop ΔP is expressed as a function of CSF seepage ψ, permeability k_{darcy}, absorption coefficient k_{abs} and ventricle radial position R_i. It is shown in Fig. 3 that among these four parameters, CSF seepage and permeability play the most important role. As the differential Biot's equations depend on the internal radius and involve large deformations in case of NPH ventricle dilation, they are iterated to reach a convergency. In other words, incremental small deformation problems are solved successively to obtain a self-consistent large deformation stable solution.

A stable ventricle geometry or equilibrium position is defined when the solution of the Biot's problem yields a zero displacement at the internal radial position, R_i. These equilibrium positions are searched for both healthy and NPH brains while the transparenchymal pressure drop remains at a low level, typically lower than 1 mm Hg, as consistently reported in experimental studies.

4.1 Influence of CSF Seepage and Permeability on Transparenchymal Pressure Drop. The pressure difference between the ventricles and the pia, ΔP defined in Eq. (14), is proportional to the magnitude of CSF seepage, ψ, and highly depends on the Darcy's permeability of the brain parenchyma. The internal radius and the absorption coefficient k_{abs} are of secondary importance. Most of the CSF entering the brain parenchyma is absorbed by the blood system but a small proportion can flow out the parenchyma towards the pia layer. This fact is used to assess values for the absorption coefficient as they are not available in literature. Values within the range 10^{-11} to 10^{-8} m^2/Ns were retained. An increase in k_{darcy} and R_i and to a less extent in k_{abs} can combine with an increase in ψ in order to keep the pressure gradient at its low level. During the NPH course, a disruption of the ependymal layer is observed as the ventricle surface is stretched. This leads to a substantial increase in the permeability which furthermore permits an increase of CSF seepage while keeping the pressure gradient to a low level.

4.2 Healthy Equilibrium Position. The relationship between absorption coefficient k_{abs}, Darcy's permeability k_{darcy} and ventricular CSF seepage ψ is derived from Eq. (14) by fixing R_i to its initial value of 2 cm, i.e., by suppressing any possible ventricle dilation. This is referred as the stability or equilibrium condition where the ventricle radial displacement remains to zero. As the transparenchymal pressure drop can amount to 1 mm Hg, CSF can increase up to 5% of the total CSF production rate, 10^{-8} m^3/s, without distorting the ventricle, as reported in Fig. 3. Besides owing to the pressure drop, the parenchyma is slightly deformed in tension in the periventricular region and in compression closer to the skull. Nevertheless, the maximum radial displacement is around 60 μm and is negligible. As long as CSF seepage does not exceed 5% of its total production and other biomechanical parameters do not change, the brain remains in its equilibrium position as this situation corresponds to the steady state solution of the Biot's equations.

4.3 NPH Equilibrium Position. When CSF seepage exceeds 5% of its total production, then a second equilibrium position corresponding to NPH condition is reached. The converged solution

for this situation is reported in Fig. 4 where CSF seepage is increased up to 10% of its total production, and yields a value of 3 cm for the internal radius. This corresponds to a rather large ventricle dilation, with a maximum radial displacement of 1 cm and is to be linked with the very beginning or onset of NPH conditions. Indeed, the high straining of the brain parenchyma yields to large volume changes as reported in Fig. 5 that will affect primarily the permeability coefficient. Indeed, it has been reported by Ref. [24], that Darcy's permeability increases exponentially with local volumetric change, i.e., with the trace of the strain tensor. As this last one depends on the radial position (cf. Figure 5(*b*)), our analytical solution is no longer valid and numerical analysis should be used instead. Qualitatively, the increase in permeability induced by the straining of the parenchyma in the periventricular zone allows for a further increase in CSF seepage without affecting the pressure drop, as shown in Fig. 7. Most important in that case is that the NPH equilibrium position remains almost constant while both permeability and CSF seepage increase. This is to be linked with NPH arrest conditions for which ventricle dilation does no longer vary. Besides, Fig. 6 shows that an increase in the ability of blood vessels to absorb CSF within the parenchyma has a slight beneficial effect in reducing both the ventricle dilation and the pressure drop. But in reality, the absorption coefficient is reported by Momjian et al. [30] to decrease in compressed areas, similarly to the Darcy coefficient.

4.4 Comparison With In vivo Facts. In NPH and in ageing, there is evidence for both an alteration in CSF production and a decrease in the CSF absorption [31–33]. Even the CSF secretion is shown to be impaired in experimentally induced hydrocephalus using kaolin [34]. A decrease in central blood flow in chronic hydrocephalus and NPH was reported by Refs. [35] and [30]. A similar decrease in white matter blood flow has also been reported in the experimentally kaolin induced chronic hydrocephalus in rats [36]. In a Dutch study on 101 NPH patients, the role of vascular disease was highlighted by Ref. [37] who found out that the proportion of patients who responded to shunt placement was significantly lower among patients with cerebrovascular disease. In idiopathic NPH cases, cerebral small vessel disease, might be the initial pathological process leading to NPH [30]. With aging, the arterioles in the deep white matter close down, leading to deep white matter ischemia noted so frequently in elderly patients and with greater frequency in NPH patients [38]. The decrease in the level of absorption can be due to the cerebral diseases while the increase in CSF flux is likely related to the alteration of the ependymal cell or the variation in the resistance of normal CSF pathways.

Our calculations are consistent with these experimental facts and support the idea that the increase in the CSF seepage through the ventricle wall and the decrease in the absorption coefficient result in a new stable position of brain with enlarged ventricles. The dilatation of ventricles occurs in the vicinity of normal transparenchymal pressure drop, prompting the NPH condition. The brain ventricles get a different stable position where the rate of absorption is close to the level of CSF seepage. This justifies why the flux controlled shunting has a better efficiency. In a study [39] and also suggested by Silverberg in his review paper [40], low-pressure valves (LPV) were shown to have a better efficiency in shunt placement than the medium pressure valves (MPV). LPV shunts provide a higher flow rates with an increase in the CSF turnover. In addition, the periventricular region is shown to be in expansion and might explain some accumulation of CSF in that region. This localized amount of fluid close to ventricular wall, leading to edema, has been observed experimentally [15,20,41].

Figure 8(*a*) shows the evolution versus time of the ventricle enlargement in percentage from the initial volume in an experimental study on monkey brains carried out by [42]. In this study, hydrocephalus was induced by the surgical obstruction of the fourth ventricle and caudal aqueduct. It is concluded by the authors that the structural and permeability changes in periventricular region are the reason for the variation of enlargement rate

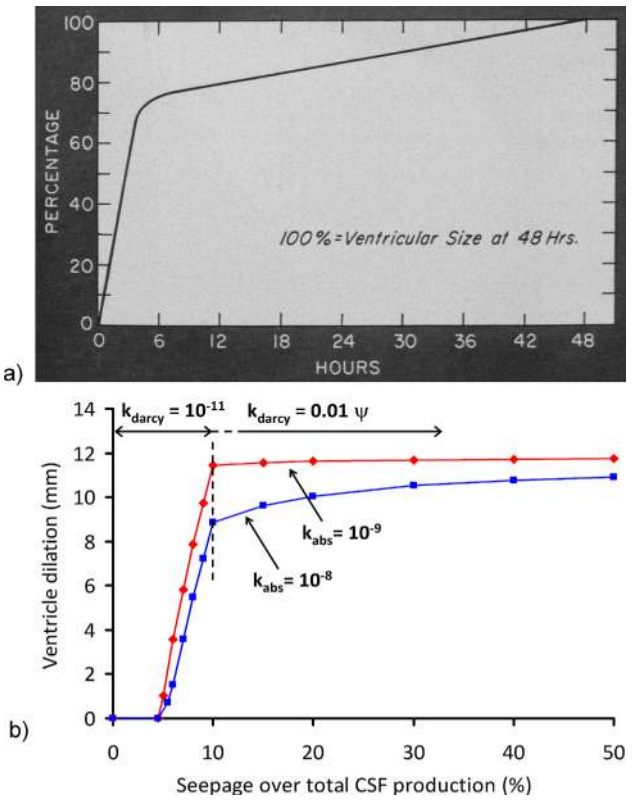

Fig. 8 (*a*) Rate of ventricular enlargement in an experimental study of hydrocephalus induced by surgical obstruction of the fourth ventricle and caudal aqueduct [42] and (*b*) ventricle dilation versus seepage predicted by the simulation

which favors the equilibration. After a rather steep increase during the first three hours, the ventricle dilation continues to increase but at a much smaller rate. This evolution is very much similar to our simulation results, notably those reported in Fig. 7 and repeated in Fig. 8(*b*): the enlargement of ventricles tends to saturate as the increase of the Darcy permeability induced by the straining of the parenchyma allows for a higher CSF seepage and flow through the brain parenchyma.

The study by Shulyakov et al. [43] evaluates the variation of biomechanical parameters of brain with maturation. They have shown that the aging evidently affects the stiffness of the brain which is likely related to the fact that brain is loosing water in older rats. To relate this issue with our model, if the brain losses water, the Darcy's permeability decreases and this affects the stability positions. Because the increase in the Darcy value favors the equilibrium position or prevents the ventricle of further enlargement. Therefore, if this coefficient decreases, like the absorption coefficient, the ventricle might enlarge as the ratio of Darcy and absorption coefficients (indicated by $k = k_{darcy}/k_{abs}$) is an important parameter in the analytical solution. Another conclusion by Shulyakov et al. is that in the case where the stress is applied repeatedly or in a pulsatile manner, there can be an accumulation of strains. This might play an important role in the presence of a CSF pulsatile component, leading to a large accumulation of strains and hydrocephalus evolution. That is something to be checked in future studies.

4.5 Role of Ependyma in NPH Development. The ependyma consisting of a thin cellular layer over the ventricular wall might have an important influence on the onset and evolution of NPH. Recently it was found that the ependymal cells also contributes to the CSF production as they are placed in the vicinity of the choroid plexus, the major site of CSF production [44]. This region

is reported to have a lower permeability as it is packed and covers the ventricles [24]. Ependymal cells also give rise to the epithelial layer that surrounds the choroid plexus, a network of blood vessels located in the walls of the lateral ventricles [45]. During NPH evolution, the ventricle surface is stretched which causes the spacing between ependyma cells to increase. Therefore, the permeability of this layer is subject to increase and to let more CSF seep towards the parenchyma and accentuate the transition towards the NPH equilibrium position.

4.6 Role of CSF Production Rate. The ratio of CSF seepage over total CSF production is an important factor in the stability position of the ventricular wall. In elderly people, the total CSF production is reported to decrease therefore if the amount of CSF seepage entering the parenchyma remains constant; this evidently leads to the ventricle enlargement in the vicinity of normal pressure. However, when the CSF production decreases, the absolute amount of seepage likely does the same. Therefore, only for the cases where the total CSF production variation does not modify the amount of CSF seepage, the ventricles will divert from the stability as the seepage ratio increases.

4.7 Comparison With Mathematical Models. Contrary to previous studies [15,22,24,26,46,47], the concept of equilibrium position is introduced starting from healthy brain and migrating towards NPH conditions. The role of the amount of CSF seepage is taken into account instead of simply applying a pressure boundary condition on the ventricle walls. The equations are solved to have a self consistent solution where the CSF seepage and ventricle wall position do no longer change. It is demonstrated that the equilibrium positions are constrained by a relationship between different biomechanical parameters such as the absorption coefficient, the Darcy permeability and the elastic constants of the parenchyma. These parameters are linked together in order to satisfy the low transparenchymal pressure drop. Among them, CSF seepage and Darcy permeability are the most influencing ones. Of course, the geometry of the brain has been oversimplified to get analytical solutions of the equations but the same equilibrium positions might appear in the 3D model as the NPH mechanism is likely not dependent on the geometry. The influence of the local volume change in the permeability requires the use of more sophisticated numerical schemes and the consideration of realistic brain geometry is under progress using finite element techniques.

4.8 Limitations. In the present study, we elaborated on and refined Levine's model to study specifically the role of CSF seepage and parenchymal absorption. Nevertheless, the accuracy of the model is evidently increased by adding the detailed geometry of aqueduct of Sylvius as well as the third and fourth ventricles. The solution then requires a numerical finite element solver. A higher threshold value is predicted for the both normal and NPH in a detailed geometry. The comparison of the ventricular surfaces in a detailed geometry ($\sim$0.014587 m^2) and the spherical model (0.005 m^2) might evidence this respective increase over the required seepage value. The ventricular and parenchymal volumes in a detailed 3D geometry and the spherical model are almost similar. However, the ventricular surface area in a detailed geometry is almost double. Therefore, in the 3D brain, the amount of seepage should be higher to have similar effects. However, this needs further numerical proof. The future analytical study should consider as well the nonrigidity of pia layer. In this case, the pia layer is no longer considered to be fixed. Therefore, instead of applying the zero displacement boundary condition on the pia layer, the normal stress confines the displacement. Giving a degree of freedom to the pia layer would in fact favor the ventricle enlargement and evidently change the equilibrium positions. In the presented study, the stress-strain nonlinearity of brain tissue was not considered. However, this aspect should be included in the future studies by incorporating more elaborated constitutive equations which further requires FE solvers to obtain the equilibrium positions of ventricle wall. Nonetheless, the brain tissue during the CSF seepage increase might present a linear behavior. If the CSF seepage increases gradually, the brain tissue reaches step by step the equilibrium positions which allow the brain tissue to adapt itself to the resulting configuration, known as stress-reduced remodelling effect.

5 Conclusion

A simple but realistic model of brain parenchyma is proposed by solving Biot's equations assuming spherical geometries for both ventricle and skull. Equilibrium positions are calculated for healthy and NPH conditions that are characterized by a normal pressure distribution throughout the parenchyma. Using a transparenchymal pressure drop of 1 mm Hg, it is shown that under healthy conditions, a small proportion, around 5% of the total CSF secreted by the choroid plexus can flow towards the brain parenchyma without leading to ventricle dilation and be absorbed partially by the blood venous system. If for any reasons, e.g., because of the presence of a tiny obstruction or increase of flow resistance in the normal CSF pathways, the amount of CSF seepage gets larger than 5% of its total production within the ventricles, the ventricle geometry migrates to another equilibrium position corresponding to NPH conditions while keeping the transparenchymal pressure drop to 1 mm Hg. Both healthy and NPH equilibrium positions are constrained by a simple mathematical relationship between different biomechanical parameters such as absorption coefficient, Darcy permeability and elastic constants of the parenchyma but among them, Darcy permeability is the most influencing one. As brain parenchyma becomes highly stretched in the periventricular region, Darcy permeability increases and the brain parenchyma can then accept more CSF without further dilating. Although the brain geometry has been oversimplified and brain plasticity ignored, the present model is able to predict the onset and development of NPH conditions starting from healthy conditions and highlight the important role of Darcy permeability in the development of NPH.

Acknowledgment

The financial support of Swiss National Fund (SNF) Grant No. 205321 is gratefully acknowledged.

Appendix

The radial displacement solution is presented in the following sentences

$$u_r(r) = \mathbf{C_1} r + \frac{\mathbf{C_2}}{r^2} - \frac{\left(F_1(r) - \frac{1}{r^2\sqrt{k}}(F_2(r) + F_3(r) + F_4(r))\right)}{6G(ad - bc)(1 - \nu)}$$

where the constants $\mathbf{C_1}$ and $\mathbf{C_2}$ are obtained from the boundary conditions:

$$\mathbf{C_1} = \frac{(b_2 a_3 - b_1 b_3)}{a_1 b_2 - a_2 b_1}$$

$$\mathbf{C_2} = \frac{(a_1 b_3 - a_2 a_3)}{a_1 b_2 - a_2 b_1}$$

where the constants a_1, a_2, a_3 and b_1, b_2, b_3 are:

$$a_1 = 2G - \frac{6G\nu}{2\nu - 1} \qquad a_2 = R_e$$

$$b_1 = -\frac{4G}{R_i^3} \qquad b_2 = \frac{1}{R_e^2}$$

$$a_3 = \frac{1}{R_i(ad-bc)}\left(\alpha(\partial p/\partial r)_{r=R_i}\left(a\cosh\left(\frac{R_i}{\sqrt{k}}\right) - b\sinh\left(\frac{R_i}{\sqrt{k}}\right)\right)\right.$$
$$- \alpha c\Delta p\cosh\left(\frac{R_i}{\sqrt{k}}\right) + \alpha d\Delta p\sinh\left(\frac{R_i}{\sqrt{k}}\right) - R_i p_{vent}(ad-bc)$$
$$\times(1-\alpha)2\alpha(ad-bc)\left(2k(\partial p/\partial r)_{r=R_i} - R_i\Delta p\right)$$
$$\left. + \frac{2(\partial p/\partial r)_{r=R_i}\alpha k(ad-bc)}{(\nu-1)}\right)$$

$$b_3 = \frac{-\alpha\sqrt{k}(2\nu-1)}{2GR_e^2(ad-bc)(\nu-1)}\left(R_e\Delta p\left(d\cosh\left(\frac{R_e}{\sqrt{k}}\right) - c\sinh\left(\frac{R_e}{\sqrt{k}}\right)\right)\right.$$
$$- \sqrt{k}\Delta p\left(d\sinh\left(\frac{R_e}{\sqrt{k}}\right) - c\cosh\left(\frac{R_e}{\sqrt{k}}\right)\right)$$
$$- \sqrt{k}(\partial p/\partial r)_{r=R_i}\left(a\cosh\left(\frac{R_e}{\sqrt{k}}\right) - b\sinh\left(\frac{R_e}{\sqrt{k}}\right)\right)$$
$$\left.\times R_e(\partial p/\partial r)_{r=R_i}\left(a\sinh\left(\frac{R_e}{\sqrt{k}}\right) - b\cosh\left(\frac{R_e}{\sqrt{k}}\right)\right)\right)$$

And the functions F_m, $m = 1, 2, ..4$ are written as follow:

$$F_1(r) = \alpha\cosh\left(\frac{r}{\sqrt{k}}\right)(2\nu-1)\left(a(\partial p/\partial r)_{r=R_i} - c\Delta p\right)$$
$$- \alpha\sinh\left(\frac{r}{\sqrt{k}}\right)(2\nu-1)\left(b(\partial p/\partial r)_{r=R_i} - d\Delta p\right)$$

$$F_2(r) = 3\alpha k\sqrt{k}\cosh\left(\frac{r}{\sqrt{k}}\right)(2\nu-1)\left(a(\partial p/\partial r)_{r=R_i} - c\Delta p\right)$$
$$- 3\alpha k\sqrt{k}\sinh\left(\frac{r}{\sqrt{k}}\right)(2\nu-1)\left(b(\partial p/\partial r)_{r=R_i} - d\Delta p\right)$$

$$F_3(r) = \alpha\sqrt{k}r^2\cosh\left(\frac{r}{\sqrt{k}}\right)(2\nu-1)\left(a(\partial p/\partial r)_{r=R_i} - c\Delta p\right)$$
$$- \alpha\sqrt{k}r^2\sinh\left(\frac{r}{\sqrt{k}}\right)(2\nu-1)\left(b(\partial p/\partial r)_{r=R_i} - d\Delta p\right)$$

$$F_4(r) = 3\alpha kr\cosh\left(\frac{r}{\sqrt{k}}\right)(2\nu-1)\left(b(\partial p/\partial r)_{r=R_i} - d\Delta p\right)$$
$$- 3\alpha kr\sinh\left(\frac{r}{\sqrt{k}}\right)(2\nu-1)\left(a(\partial p/\partial r)_{r=R_i} - c\Delta p\right)$$

References

[1] Shapiro, K., Kohn, I. J., Takei, F., and Zee, C., 2009, "Progressive Ventricular Enlargement in Cats in the Absence of Transmantle Pressure Gradients," J. Neurosurg., **67**(1), pp. 88–92.

[2] Stephensen, H., Tisell, M., and Wikkelsö, C., 2002, "There is no Transmantle Pressure Gradient in Communicating or Noncommunicating Hydrocephalus," Neurosurgery, **50**(4), pp. 763–773.

[3] Linninger, A. A., Xenos, M., Zhu, D. C., Somayaji, M. R., Kondapalli, S., and Penn, R. D., 2007, "Cerebrospinal Fluid Flow in the Normal and Hydrocephalic Human Brain," IEEE Trans. Biomed. Eng. **54**(2), pp. 291–302.

[4] Levine, D. N., 2008, "Intracranial Pressure and Ventricular Expansion in Hydrocephalus: Have we Been Asking the Wrong Question?" J. Neurol. Sci., **269**(1-2), pp. 1–11.

[5] Linninger, A., Sweetman, B., and Penn, R., 2009, "Normal and Hydrocephalic Brain Dynamics: The Role of Reduced Cerebrospinal Fluid Reabsorption in Ventricular Enlargement," Ann. Biomed. Eng., **37**(7), pp. 1434–1447.

[6] Matsumoto, T., Nagai, H., Kasuga, Y., and Kamiya, K., 1986, "Changes in Intracranial Pressure (ICP) Pulse Wave Following Hydrocephalus," Acta Neurochir., **82**(1), pp. 50–56.

[7] Penn, R. D., Lee, M. C., Linninger, A. A., Miesel, K., Lu, S. N., and Stylos, L., 2005, "Pressure Gradients in the Brain in an Experimental Model of Hydrocephalus," J. Neurosurg., **102**(6), pp. 1069–1075.

[8] Penn, R. D., and Linninger, A., 2009, "The Physics of Hydrocephalus," Pediatr. Neurosurg., **45**(3), pp. 161–174.

[9] Børgesen, S. E., 1984, "Conductance to Outflow of CSF in Normal Pressure Hydrocephalus," Acta Neurochir., **71**(1), pp. 1–45.

[10] Bateman, G. A., 2000, "Vascular Compliance in Normal Pressure Hydrocephalus," AJNR Am. J. Neuroradiol., **21**(9), pp. 1574–1585.

[11] Tullberg, M., Jensen, C., Ekholm, S., and Wikkelso, C., 2001, "Normal Pressure Hydrocephalus: Vascular White Matter Changes on MR Images Must Not Exclude Patients from Shunt Surgery," AJNR Am. J. Neuroradiol., **22**(9), pp. 1665–1673.

[12] Sobey, I., and Wirth, B., 2006, "Effect of Non-Linear Permeability in a Spherically Symmetric Model of Hydrocephalus," IMA J. Math Appl. Med. Biol., **23**(4), pp. 339–361.

[13] Hamlat, A., Adn, M., Sid-ahmed, S., Askar, B., and Pasqualini, E., 2006, "Theoretical Considerations on the Pathophysiology of Normal Pressure Hydrocephalus (NPH) and NPH-Related Dementia," Med. Hypotheses, **67**(1), pp. 115–123.

[14] Nagashima, T., Tamaki, N., Matsumoto, S., Horwitz, B., and Seguchi, Y., 1987, "Biomechanics of Hydrocephalus: A New Theoretical Model," Neurosurgery, **21**(6), pp. 898–904.

[15] Levine, D., 1999, "The Pathogenesis of Normal Pressure Hydrocephalus: A Theoretical Analysis," Bull. Math. Biol., **61**(5), pp. 875–916.

[16] Marmarou, A., Shulman, K., and LaMorgese, J., 1975, "Compartmental Analysis of Compliance and Outflow Resistance of the Cerebrospinal Fluid System," J. Neurosurg., **43**(5), pp. 523–534.

[17] Linninger, A., Xenos, M., Sweetman, B., Ponkshe, S., Guo, X., and Penn, R., 2009, "A Mathematical Model of Blood, Cerebrospinal Fluid and Brain Dynamics," J. Math. Biol., **59**(6), pp. 729–759.

[18] Levine, D. N., 2000, "Ventricular Size in Pseudotumor Cerebri and the Theory of Impaired CSF Absorption," J. Neurol. Sci., **177**(2), pp. 85–94.

[19] Franceschini, G., Bigoni, D., Regitnig, P., and Holzapfel, G. A., 2006, "Brain Tissue Deforms Similarly to Filled Elastomers and Follows Consolidation Theory," J. Mech. Phys. Solids, **54**(12), pp. 2592–2620.

[20] Hopkins, L. N., Bakay, L., Kinkel, W. R., and Grand, W., 1977, "Demonstration of Transventricular CSF Absorption by Computerized Tomography," Acta Neurochir., **39**(3), pp. 151–157.

[21] Smillie, A., Sobey, I., and Molnar, Z., 2005, "A Hydroelastic Model of Hydrocephalus," J. Fluid Mech., **539**(1), pp. 417–443.

[22] Momjian, S., and Bichsel, D., 2006, "Elastic and Poro-Elastic Models of Ventricular Dilatation in Hydrocephalus," COMSOL Users Conference, Grenoble.

[23] Shahim, K., Drezet, J.-M., Molinari, J.-F., Sinkus, R., and Momjian, S., 2010, "Finite Element Analysis of Normal Pressure Hydrocephalus: Influence of CSF Content and Anisotropy in Permeability," J. Appl. Biomater. Biomech., **7**(3), pp. 187–197.

[24] Kaczmarek, M., Subramaniam, R., and Neff, S., 1997, "The Hydromechanics of Hydrocephalus: Steady-State Solutions for Cylindrical Geometry," Bull. Math. Biol., **59**(2), pp. 295–323.

[25] Biot, M. A., 1941, "General Theory of Three-Dimensional Consolidation," J. Appl. Phys., **12**(2), pp. 155–164.

[26] Hakim, S., Venegas, J. G., and Burton, J. D., 1976, "The Physics of the Cranial Cavity, Hydrocephalus and Normal Pressure Hydrocephalus: Mechanical Interpretation and Mathematical Model," Surg. Neurol., **5**(3), pp. 187–210.

[27] Wirth, B., 2005, "A Mathematical Model for Hydrocephalus," M.S. thesis, University of Oxford, St. Anne's College, University of Oxford.

[28] Green, M. A., Bilston, L. E., and Sinkus, R., 2008, "In vivo Brain Viscoelastic Properties Measured by Magnetic Resonance Elastography," NMR Biomed., **21**(7), pp. 755–764.

[29] Gideon, P., Ståhlberg, F., Thomsen, C., Gjerris, F., Sørensen, P. S., and Henriksen, O., 1994, "Cerebrospinal Fluid Flow and Production in Patients with Normal Pressure Hydrocephalus Studied by MRI," Neuroradiology, **36**(3), pp. 210–215.

[30] Momjian, S., Owler, B. K., Czosnyka, Z., Czosnyka, M., Pena, A., and Pickard, J. D., 2004, "Pattern of White Matter Regional Cerebral Blood Flow and Autoregulation in Normal Pressure Hydrocephalus," Brain, **127**(5), pp. 965–972.

[31] Silverberg, G. D., Huhn, S., Jaffe, R. A., Chang, S. D., Saul, T., Heit, G., Von Essen, A., and Rubenstein, E., 2002, "Downregulation of Cerebrospinal Fluid Production in Patients with Chronic Hydrocephalus," J. Neurosurg., **97**(6), pp. 1271–1275.

[32] Czosnyka, M., Whitehouse, H., Smielewski, P., Simac, S., and Pickard, J. D., 1996, "Testing of Cerebrospinal Compensatory Reserve in Shunted and Non-Shunted Patients: A Guide to Interpretation Based on an Observational Study," J. Neurol., Neurosurg. Psychiatry, **60**, pp. 549–558.

[33] May, C., Kaye, J. A., Atack, J. R., Schapiro, M. B., Friedland, R. P., and Rapoport, S. I., 1990, "Cerebrospinal Fluid Production is Reduced in Healthy Aging," Neurology, **40**(1), pp. 500–503.

[34] Marlin, A. E., Wald, A., Hochwald, G. M., and Malhan, C., 1978, "Kaolin-Induced Hydrocephalus Impairs CSF Secretion by the Choroid Plexus," Neurology, **28**(9), pp. 945–949.

[35] Dombrowski, S. M., Schenk, S., Leichliter, A., Leibson, Z., Fukamachi, K., and Luciano, M. G., 2006, "Chronic Hydrocephalus-Induced Changes in Cerebral Blood Flow: Mediation Through Cardiac Effects," J. Cereb. Blood Flow Metab., **26**(10), pp. 1298–1310.

[36] Klinge, P. M., Samii, A., Muhlendyck, A., Visnyei, K., Meyer, G.-J., Walter, G. F., Silverberg, G. D., and Brinker, T., 2003, "Cerebral Hypoperfusion and Delayed Hippocampal Response After Induction of Adult Kaolin Hydrocephalus," Stroke, **34**(1), pp. 193–199.

[37] Boon, A. J. W., Tans, J. T. J., Delwel, E. J., Egeler-Peerdeman, S. M., Hanlo, P. W., Wurzer, H. A. L., and Hermans, J., 1999, "Dutch Normal-Pressure Hydrocephalus Study: The Role of Cerebrovascular Disease," J. Neurosurg., **90**(2), pp. 221–226.

[38] Bradley, W., Jr., Whittemore, A., Watanabe, A., Davis, S., Teresi, L., and Homyak, M., 1991, "Association of Deep White Matter Infarction with Chronic Communicating Hydrocephalus: Implications Regarding the Possible Origin of Normal-Pressure Hydrocephalus," AJNR Am. J. Neuroradiol., **12**(1), pp. 31–39.

[39] Boon, A. J. W., Tans, J. T. J., Delwel, E. J., Egeler-Peerdeman, S. M., Hanlo, P. W., Wurzer, H. A. L., Avezaat, C. J. J., de Jong, D. A., Gooskens, R. H. J. M.,

and Hermans, J., 1998, "Dutch Normal-Pressure Hydrocephalus Study: Randomized Comparison of Low- and Medium-Pressure Shunts," J. Neurosurg., **88**(3), pp. 490–495.
[40] Silverberg, G. D., 2004, "Normal Pressure Hydrocephalus (NPH): Ischaemia, CSF Stagnation or Both," Brain, **127**(5), pp. 947–948.
[41] Naidich, T. P., Epstein, F., Lin, J. P., Kricheff, I. I., and Hochwald, G. M., 1976, "Evaluation of Pediatric Hydrocephalus by Computed Tomography," Radiology, **119**(2), pp. 337–345.
[42] Milhorat, T. H., Clark, R. G., Hammock, M. K., and McGrath, P. P., 1970, "Structural, Ultrastructural, and Permeability Changes in the Ependyma and Surrounding Brain Favoring Equilibration in Progressive Hydrocephalus," Arch. Neurol., **22**(5), pp. 397–407.
[43] Shulyakov, A. V., Cenkowski, S. S., Buist, R. J., and Del Bigio, M. R., 2011, "Age-Dependence of Intracranial Viscoelastic Properties in Living Rats," J. Mech. Behav. Biomed. Mater., **4**(3), pp. 484–497.
[44] Welch, K., 1963, "Secretion of Cerebrospinal Fluid by Choroid Plexus of the Rabbit," Am. J. Physiol., **205**(3), pp. 617–624.
[45] Del Bigio, M. R., 1995, "The Ependyma: A Protective Barrier Between Brain and Cerebrospinal Fluid," Glia, **14**(1), pp. 1–13.
[46] Dutta-Roy, T., Wittek, A., and Miller, K., 2008, "Biomechanical Modelling of Normal Pressure Hydrocephalus," J. Biomech., **41**(10), pp. 2263–2271.
[47] Peña, A., Harris, N., Bolton, M., Czosnyka, M., and Pickard, J., 2002, "Communicating Hydrocephalus: The Biomechanics of Progressive Ventricular Enlargement Revisited," Acta Neurochir. Suppl. (Wien) **81**, pp. 59–63.